



Improved cationic dye removal from aqueous solutions using sawdust treated with zinc nanoparticles

*Elbadry A. Elbadry**, *M. A. Hashem*, *Amira L. Shafik*

Department of Chemistry, Faculty of Science, Mansoura University

* *Corresponding author: elbadryahmed961@gmail.com, Tel 01123506518*

Received: 27/4/2024
Accepted: 29/4/2024

Abstract: Chemically modified sawdust zinc nanoparticles (MC/Zn-NPs) were created and examined utilizing a number of specialized methods, including energy-dispersive X-ray spectroscopy (EDX), FT-IR, BET, and scanning electron microscopy. The MC/Zn-NPs that were created were utilized to absorb various organic dyes from different sources, including crystal violet, methylene blue, and malachite green dye. The ideal sorption conditions have been determined through examining sorption parameters such as pH, temperature, sorption period, and sorbent concentration. The second-order model was in agreement with the sorption kinetics, and the chemical adsorption is the rate-limiting step. Additionally, the sorption isotherm experiments showed that 180, 250, and 210 mg/g of crystal violet, methylene blue, and malachite green dye, respectively, were the best acceptable with Langmuir model sorption uptake of (MC/Ag-NPs). Crystal violet, methylene blue, and malachite green dye were among the actual samples that were utilized for analytical applications with the current methodology, and the results show promise.

keywords: Sawdust. Dialdehyde Cellulose. Periodate oxidation. Zinc nanoparticles. Adsorption.

1.Introduction

The upkeep of the natural environment is facing an unavoidable problem due to the proliferation of manufacturing activities over the past few decades, which has resulted in water pollution from many sources, particularly dye wastewater[1]. Large amounts of wastewater are produced when 10% to 30% of the colors used in textile dyeing are later thrown away because of their weak affinity for the textile fiber composition. Chemicals such as benzene, naphthalene, anthraquinone, aniline, or benzidine are included in the majority of colors. These dyes have a limited biodegradability and may be harmful to aquatic habitats and human health due to their fragrant nature[2]. Thus, it is believed that protecting the environment and public health requires effectively removing color from wastewater and disposing of it.

Recently, there has been a lot of emphasis on developing cost-effective adsorbents for wastewater treatment applications. Numerous research have been undertaken to remove dyes from wastewater utilizing agricultural leftovers

such as peanut husk, apple pomace, wheat straw, wheat shell, cereal chaff, fruit peel, bark, and leaves[3-8]. To boost the sorption capacity of a crude agricultural waste, chemical treatment was used. There is always a need for separation procedures that remove hazardous dyes from polluted water and industrial stream. Many approaches, such as ion exchange, precipitation, membrane processes, and solid phase extraction, have been utilized to eliminate pollution produced by hazardous dyes[8,9]. The economical and efficient method of removing dangerous dyes from wastewater is solid phase extraction[1, 2].

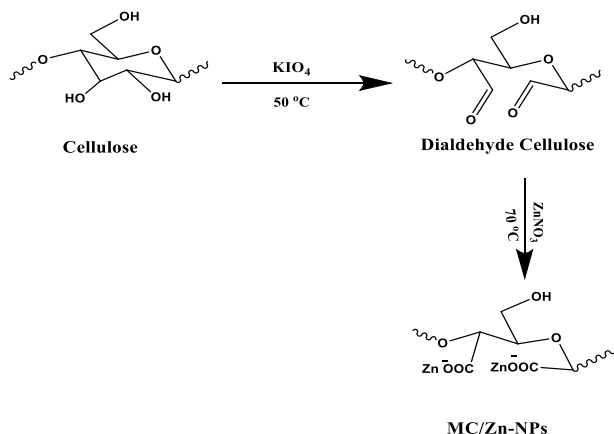
Chelating fibers, which are employed for preconcentration and removal of dangerous dyes from various polluted solutions, are being focused on due to their large adsorption capacity and high selectivity[3-5].

Cellulose is one of the most prevalent and replenishable biopolymers in the natural world. It's currently trendy to use biodegradable materials as a metal scavenger. New chelating

groups must be added to cellulose in order to change it chemically and physically and increase its capacity to scavenge metals. These changes enable the absorption of hazardous dyes by cellulose.

A byproduct of the timber industry, sawdust is expected to be generated in excess of 100 million tons, of which 96% will come from emerging nations. By using this source of agricultural waste, a disposal issue may be resolved and access to a less expensive material for adsorption in water pollution control system might be gained.

In this instance, lignin is eradicated from sawdust by treating it with a NaOH solution. Modified sawdust (MC/Zn-NPs) is the result of treating dialdehyde cellulose (DAC) with ZnNO₃ for zinc nanoparticle (Zn-NPs) donation after an aldehyde group is added by an oxidation process with potassium periodate. (MC/Zn-NPs) have the potential to eliminate cationic dyes such as crystal violet, methylene blue, and malachite green from wastewater after optimization.



Scheme 1: Preparation of MC/Zn-NPs

2. Materials and methods

2.1. Materials

Hardwood sawdust with particle sizes between 0.5 and 1.0 μm was collected, sieved, and utilized for the investigations from a neighboring furniture workshop [5]. Potassium periodate, zinc nitrate, sodium hydroxide, crystal violet (CV), methylene blue (MB), and malachite green (MG) were purchased from sigma Aldrich. No pre-treatment was applied before using any of the bought chemicals. To make a stock (1000 ppm) of each dye, one gram of each dye (MB, CV, and MG) was dissolved in one liter of redistilled water in a

1000 ml measuring flask. using a standard curve that was made from a number of dye solutions with known dye concentrations using a UV-visible spectrometer. Sawdust and deionized water were blended, sonicated, and filtered. The process was repeated until the water washings were clear. To get rid of lignin, the dry sawdust was immersed in a 200 mL, 2 M NaOH solution for a whole day. After that, it was cleaned with deionized water, immersed in a 200 mL solution of 1% v/v H₂SO₄, and allowed to air dry for an extra night at 50 °C in an oven. Because high drying temperatures may induce a decrease in the number of cellulose-based OH- groups on the wood's decreased moisture content, 50 °C was chosen as the drying temperature. Potassium periodate (14 g, 0.06 mole) solution was prepared by dissolving 14 g of potassium periodate in 250 ml of deionized water, which may result in a thermic deactivation of the wood surface [3,5,7].

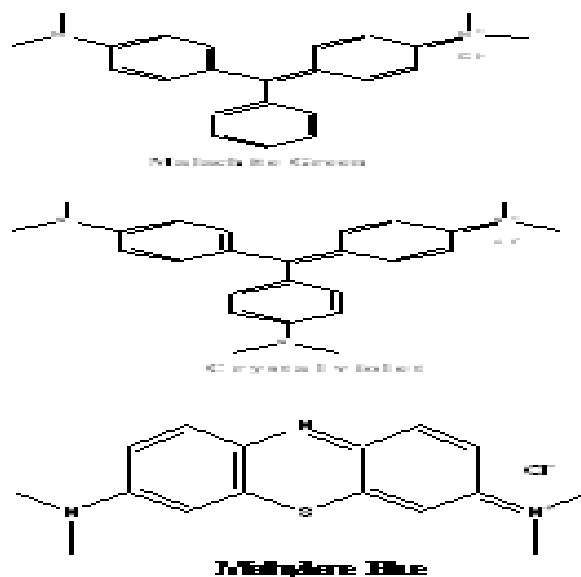


Fig.1: Chemical structures of the investigated acid dyes.

2.2. Modification of Wood

2.2.1. Dialdehyde Cellulose (DAC)

Potassium periodate was progressively added to 5 g of modified Wood that had been suspended in 50 mL of water for two hours. The combination was heated to 50°C for 24 hours in the absence of light. At temperatures higher than 55°C, periodate becomes unstable and finally decomposes to release iodine, making it challenging to estimate the real amount of periodate consumed. Ethylene glycol was then added in order to get rid of any

leftover potassium periodate. After being filtered and cleansed with distilled water, the product (DAC) was finally dried at 50°C [14,15].

2.2.2. Grafting of zinc nano-particles (MC/Zn-NPs)

Zinc nitrate solution was combined with dialdehyde sawdust (DAC), and the mixture was incubated for 24 hours at 70 °C [16]. The fibers were filtered, then repeatedly washed with deionized water and dried in an oven. ZnNO₃ reduction into Zn-NPs is visually confirmed by the reddish-brown color shift of DAC [6,7].

2.3. Characterization of samples

Morphological characterizations have been performed with a JSM-6510LV. Prior to analysis, each sample was gold sputter-coated. The infrared spectra of the materials were recorded using a Fourier transform infrared spectrometer (FT-IR) (Perkin-Elmer spectrum). A UV/Visible Unicam UV 2100 spectrometer has been used to detect the amount of dyes that have been adsorbed that remains.

2.4. Adsorption and regeneration of organic dyes

The adsorption of adsorbed dyes was achieved via batch testing. Using 250 ml bottles containing 100 ml of adsorbate solutions and an adsorbent dosage, adsorption experiments were carried out to measure the amount of remaining adsorbed colors in duplicate samples. Then, using a shaker with the temperature set to 25 degrees Celsius, the stoppered bottles were shaken at 200 revolutions per minute. The mixture's pH was adjusted with the aid of sodium hydroxide and hydrochloric acid. Upon reaching the adsorption equilibrium, the contents of the bottles were centrifuged. The quantity of liquid supernatant containing the dyes that haven't yet adsorbed was calculated. A wide range of parameters were investigated, such as temperature (20–50 °C), adsorbent dose (0.2–1 g), pH parameter (2–7), and adsorbate beginning concentration (25–250 ppm).

Eqs. 1 and 2 were used to calculate the removal effectiveness (%) respectively, and the volume of adsorbed adsorbate at equilibrium q_e (mg/g).

$$\text{Removal}\% = \frac{C_i - C_f}{C_i} \times 100 \quad \text{Eq 1}$$

$$q_e = \frac{(C_i - C_f) \cdot v}{wt} \quad \text{Eq 2}$$

where C_i (ppm) is the initial adsorbate concentration, C_f (ppm) is the equilibrium adsorbate concentration, wt (g) is the adsorbent amount, and V (L) is the volume of the adsorbate solution.

The adsorbent material (MC/Zn-NPs) was regenerate by adsorption-desorption tests. First, a batch adsorption experiment was conducted for three hours at 25°C and pH 2 using 50 ml of a solution containing 100 ppm of adsorbed dyes and 0.1 g of MC/Zn-NPs. For the desorption investigations, K₂CO₃ 0.1 M was employed as the eluent. A one-hour shaking was performed on fifty milliliters of 0.1 M solution and 0.1 gram of dye-adsorbed MC/Zn-NPs. Finally, employing the regenerating adsorbents, four further cycles of the adsorption-desorption cycle were carried out.

2.5. Preparation of actual samples

Five milliliters of 98% (w/w) H₂SO₄, 0.5 grams of potassium per sulphate, or K₂S₂O₈, and one thousand milliliters of water sample were added in order to completely break down any possible organic waste. I then heated the mixture to 95 °C for two hours. Once the sample had cooled to room temperature, 0.1 g of modified fiber was added to assure total analyte separation. After that, the pH was raised to 6.5 while being constantly stirred for 180 minutes. Next, an additional 0.1 g of modified sawdust fiber was added to the filtrate. A Unicam UV spectrometer was used to measure the amount of dyes that remained adsorbed.

The dehydrated MC/Zn-NPs were blended with a 100 ml dye solution and continuously shaken at 180 rpm. Periodically, samples were removed from the reaction mixture. The MC/Zn-NPs dye-adsorbed make precipitation possible. Using a UV-visible spectrophotometer (Perkin Elmer lambda 25 in the 300–600 nm range), the adsorption of the supernatant was judged. The residual dye concentration may be found using a standard curve that was constructed from many dye solutions with known dye concentrations.

The following Eq.1 was used to determine the amount of dyes adsorbed. where, q_e is the

adsorbed amount, C_0 and C_t are initial concentration and concentration of the adsorbate after time t , respectively, mg L^{-1} ; V is the volume of the solution, l , and m is the weight of the MC/Zn-NPs which used. The percentage removal of the dye was calculated using the following Eq.2.

Herein, the variables such as mixing duration, MC/Zn-NP weight added, dye concentration at begin and pH influence which was achieved by adjusting the pH between 2 and 7 affect the percentage removal of the dye have been evaluated.

3. Results and Discussion

3.1. Characterization

3.1.1. FTIR spectra

A new absorption band was seen at about 1735 cm^{-1} , which matched to the development of the aldehyde group ($\text{C}=\text{O}$), when the DAC spectra was compared to the unaltered oxidized spectrum (Fig. 2). This indicated that sawdust's molecular chain's hydroxyl groups had oxidized to aldehyde groups on the cellulose backbone. The O-H stretching vibration band was seen at 3352 cm^{-1} in modified sawdust and DAC. After grafting with Ag-NPs, the peak narrowed and moved to 3416 cm^{-1} due to the interaction between Zn-NPs and hydroxyl. The symmetric bending vibrations of CH_2 groups in the C6 of DAC chains were responsible for the subsequent drop in the intensity of the absorption peak at 1427 cm^{-1} . This suggested that some hydroxyl groups in the C6 of sawdust cellulose of chains were also involved in the reaction.

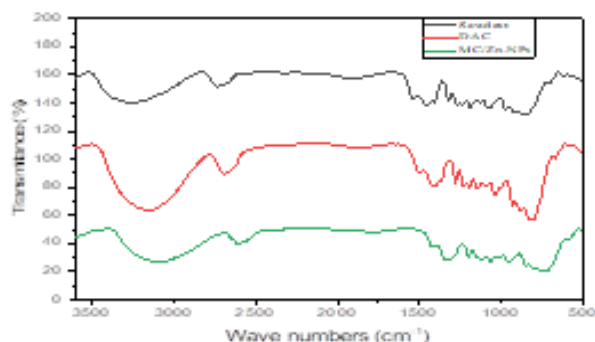


Fig.2: FT-IR spectra of Sawdust, DAC and MC/Zn-NPs

3.1.2. Brunauer-Emmett-Teller (BET)

The samples' specific surface attributes were assessed using Brunauer-Emmett-Teller (BET)

surface area analysis and Barrett-Joyner-Halenda (BJH) pore size and volume analysis. According to the BET specific surface area calculations, the MC/Zn-NPS sorbent has a surface area of $651.425 \text{ m}^2 \text{ g}^{-1}$, whereas native sawdust has a surface area of $42.341 \text{ m}^2 \text{ g}^{-1}$. The observed boost in specific surface area post chemical treatment might be taken as evidence of surface modification of sawdust by micro zinc ions. This rise is generated by covering sawdust with nano zinc, which boosts the adsorption of N_2 molecules employed in the surface area measurement procedure.

3.1.3. Point of zero charge (PZC)

Investigating the sorbate affinity to sorbent surface characterisation requires an understanding of the point of zero charge (PZC). The PZC for MC/Zn-NPS was investigated, and the pH value ranged from 2 to 9, as Figure 3 illustrates. The PZC values of the MC/Zn-NPS fibers are obtained at pH 5. The isoelectric point of the modified sawdust fiber changes as a result of the addition of zinc ions to its surface. The findings indicate that the MC/Zn-NPS fiber surface exhibits positive charges at pH values below 5, and negative signs at pH values above 6.

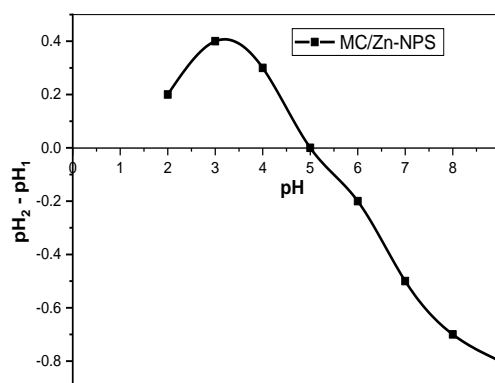


Fig. 3: The point of zero charge of (PZC) MC/Zn-NPS

3.1.4. SEM analysis

SEM photos delineated the changes in the topography of DAC and MC/Zn-NPs composite in contrast to the sawdust (Fig.4). It is showed that the surface of Sawdust very smooth, but after oxidation (DAC) there is a great change. grafting with Ag the Zn-NPs were spherical in shape with size was between 70 to 121 nm (Fig.4.d). These results confirm effective

interactions occurring by crosslinking of the Zn-NPs on DAC.

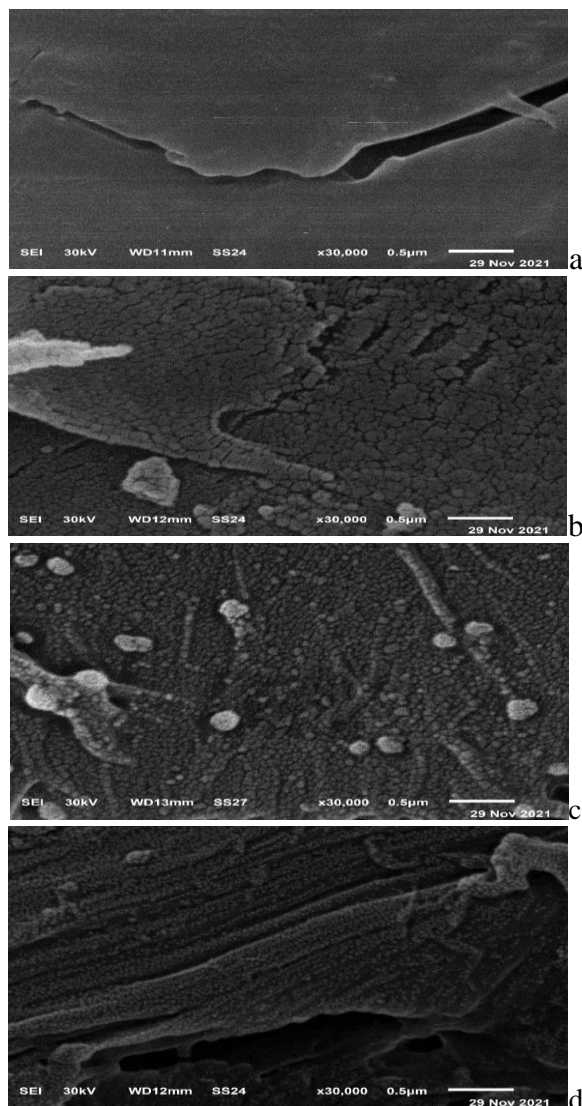


Fig.4: SEM images of (a) Sawdust, (b) oxidized Sawdust (DAC), (c) MC/Zn-NPs and (d) MC/Zn-NPs after adsorption of M.B dye.

3.1.5. E.D.X Analysis

Energy dispersive X-ray spectroscopy (EDX) reveals chemical information pertaining to a substance that align with the elemental analysis results. If an incoming electron beam hits an atom with enough energy, it might knock off one electron in the inner shell. An X-ray photon or Auger electron is emitted as the excited atom settles back into its stable state. Since the energy of the X-rays is specific to each atom, they can reveal crucial chemical details about the sample that contains metal. Based on the acquired data, the principal peaks for C and O as well as the newly observed peaks for the adsorbed silver ions on the surface of modified cellulose (Fig. 5.a, b) may

be interpreted as a reliable indicator of the DAC/Zn-NPs' production.

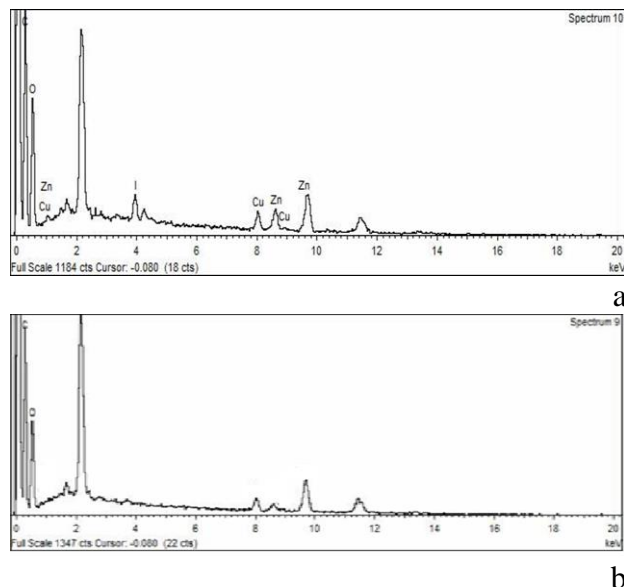


Fig.5: EDX spectrum of a. Sawdust, and b. MC/Zn-NPs.

3.2. Optimization studies

3.2.1. Effect of pH

pH is one of the most significant variables in dye adsorption, and the pH of the aqueous solution greatly affects the equilibrium [8]. At lower pH levels, the cationic dyes and H^+ ions compete for the exchange sites on the sawdust. Most cationic dyes exhibit increased adsorption within a given pH range when pH rises to a set point and subsequently decreases; other dyes lose color when pH goes over pH 9. The pH range of 2.0–7.0 was used in the current study to evaluate the dye clearance %, as shown in Fig. 6. The pH_{pzc} of MC/Zn-NPs is around 5, which is in line with the significant cationic organic dye removal at pH 6 that occurs after the formation of a negative sign on the modified surface.

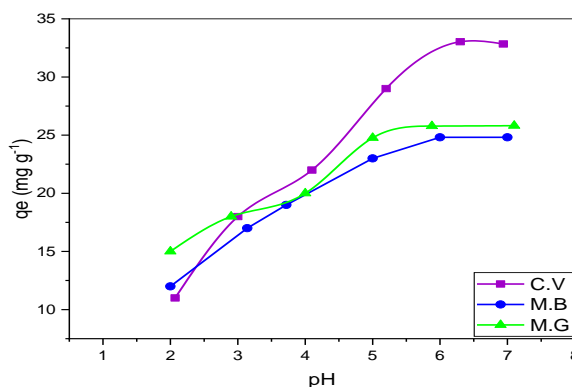


Fig.6: Effect of pH of medium on adsorption of dyes.

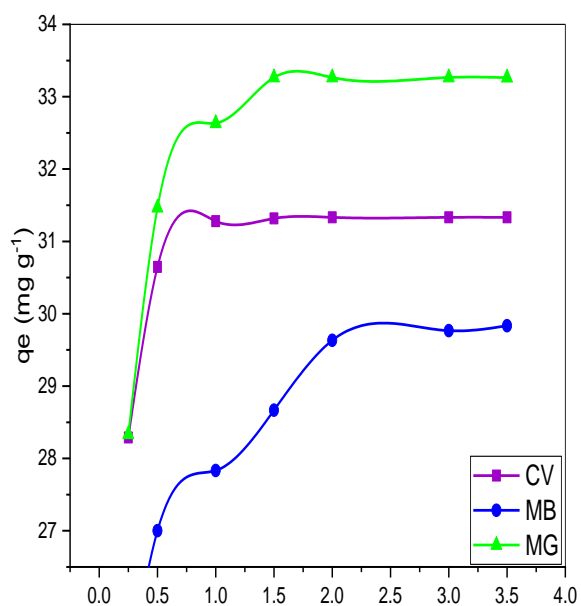


Fig.7.a: Effect of dose of MC/Zn-NPs on removal percentage.

3.2.2. Effect of adsorbent dose

In Figure 7.a Considering the impact of catalyst dosage demonstrated that, the number of photons absorbed increased in proportion to an increase in catalyst molecules, the percentage degradation of dyes CV, MB, and MG increased with increasing weight of MC/Zn-NPs and MC/Zn-NPs from 0.1 to 1 g and remained constant above 0.4 gram [8-10].

The density of the molecule in the area of illumination also increases and thus the activity gets enhanced Figure 7.b.

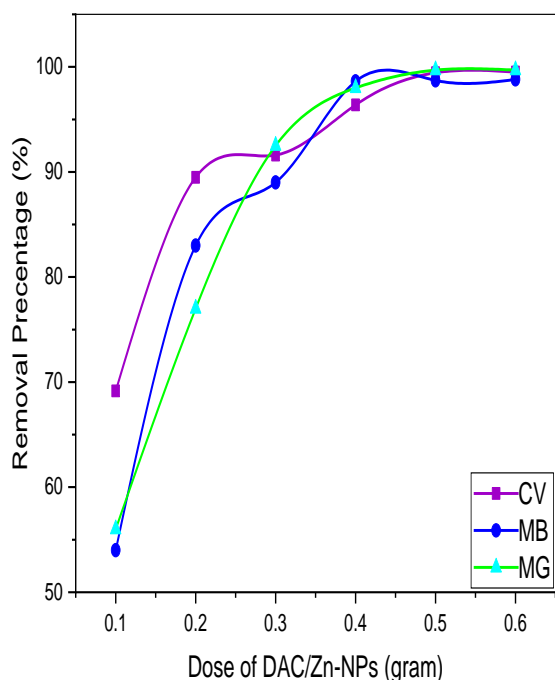


Fig.7.b: Effect of dose of MC/Zn-NPs on the maximum removal capacity.

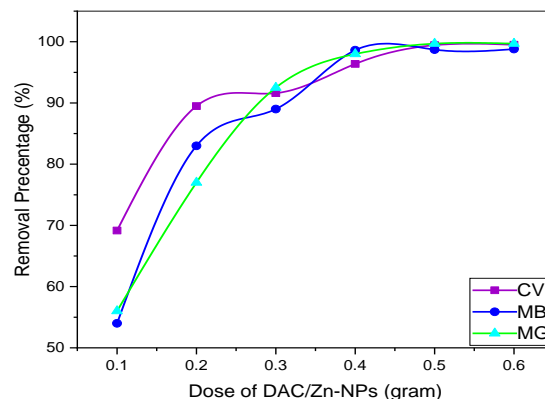


Fig.8: Influence of contact time on adsorption of dyes solution by MC/Zn-NPS.

3.2.3. Effect of contact time on removal of cationic dyes

Different amounts of 0.1 g of (MC/Zn-NPS) material were added as adsorbents to a series of bottles containing 100 ml of solutions containing 100 mg/l of adsorbed dyes at 25°C. This made it easier to examine the contact time parameter which is important to know in order to calculate sorption efficiency—at various adsorption times, from 60 to 240 minutes (fig. 8).

Planning the sorption system, better understanding the sorption process, and determining the step that influences the adsorption rate may all be facilitated by the study of kinetic factors. Multiple active functional groups allow MC/Zn-NPs to display a wide range of interactions. As demonstrated by Equation (3), An equation of the first order is a pseudo-first order one.

$$1/q_{t(ads)} = (k_1/q_{e(ads)}t) + (1/q_{e(ads)}) \quad \text{Eq.(3)}$$

$$t/q_{t(ads)} = (1/k_2q_{e(ads)}^2) + ((1/q_{e(ads)})t) \quad \text{Eq.(4)}$$

And pseudo-second order equation as in Eq. (5).

where $q_{e(ads)}$ ($\text{mg} \cdot \text{g}^{-1}$) and $q_{t(ads)}$ ($\text{mg} \cdot \text{g}^{-1}$) are the adsorption abilities at equilibrium and at time (min), respectively. K_2 is the pseudo-second-order adsorption rate constant and K_1 is pseudo-first-order sorption rate constant.

The correlation coefficient and the model that was closest to the test adsorption data were used to choose the kinetic model that best match the experimental data. The two models' K and $q_{e(ads)}$ were usually calculated simultaneously. Table (1) displays the kinetic parameters for the models that are supplied. The estimated values, $q_{e(ads)}$, utilizing pseudo-

second-order kinetic models, match the experimental values, and the correlation coefficients (R^2) are also relied upon. Because of this, the experimental kinetic data are compatible with the pseudo-second-order condition.

Table 1: Kinetic parameters for MC/Zn-NPS-mediated adsorbed dye adsorb

| Fibers | | First-order model | |
|----------------------------|--------------------|-------------------|-------|
| k_1 (min ⁻¹) | $q_{e,ads}$ (mg/g) | R^2 | |
| MC/Zn-NPs/M.B | 2.9 | 125 ± 3 | 0.925 |
| MC/Zn-NPs/C.V | 3.2 | 155 ± 2 | 0.921 |
| MC/Zn-NPs/M.G | 2.5 | 145 ± 2 | 0.891 |

| Fibers | | Second-order model | |
|--------------------|------------------------|--------------------|-------|
| k_2 (g/(mg min)) | $q_{e,ads}$ (mg/g) | R^2 | |
| MC/Zn-NPs/M.B | 2.1 × 10 ⁻³ | 166 ± 2 | 0.968 |
| MC/Zn-NPs/C.V | 2.7 × 10 ⁻³ | 140 ± 3 | 0.958 |
| MC/Zn-NPs/M.G | 2.3 × 10 ⁻³ | 154 ± 2 | 0.963 |

3.2.4. Impact of initial concentration on the capacity for adsorption

Sorbent isotherm research are essential to grasping the type of interaction between the adsorbed dyes solution and chelating fibers, as seen in figure 9. In contrast to the concentration in the bulk solution, the concentration of the dyes near the fibers' surface reduced as they were adsorbed on the MC/Zn-NPs fibers. In equilibrium, this might lead to an increase in the adsorption capacity under the defined mass transfer force. The Langmuir model is a fairly simple theoretical model for monolayer sorption onto a surface with a finite number of identical sorption sites. The Langmuir equation can be applied depending on the following fundamental presumptions: (a) molecules are adsorbed at a fixed number of well-defined localized sites; (b) each site can hold one adsorbate molecule; (c) all sites are energetically equivalent; and (d) there are no interactions between molecules adsorbed on neighboring sites.

An empirical formula applicable to both non-ideal and multiple layer adsorption on

surfaces with heterogeneous characteristics is the Freundlich expression [9, 10]. Additionally, the mathematical analysis of the isotherm has been carried out using the well-known Langmuir and Freundlich models, which are represented by Eqs. (3) and (4), respectively. [1-3]

$$\frac{C_e}{q_e} = \frac{1}{K_L q_m} + \frac{C_e}{q_m}$$

$$\ln q_e = \ln K_F + \frac{1}{n} \ln C_e$$

Eq. (3) Eq. (4)

where K_L (L/mmol) is the Langmuir model constant; K_F and n are Freundlich model constants; C_e (mmol/L) is the equilibrium dye concentration following equilibration; q_e (mmol/g) is the amount of dye concentration adsorbed by MC/Zn-NPs; and q_m (mmol/g) is the calculated maximum capacity of dye concentration by the MC/Zn-NPs adsorbent fibers.

We examined the Langmuir and Freundlich isotherm models. Table (2) displays the calculated experimental results.

The Langmuir model fits the computed experimental data the best, according to the correlation coefficient values.

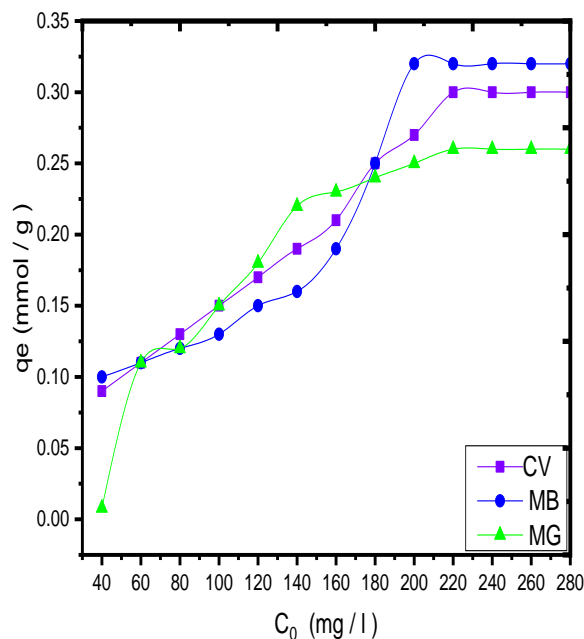


Fig.9: Adsorption isotherm of studied dyes by MC/Zn-NPs sorbents initial concentrations, at pH 6.0, and shaking rate 150 rpm, at 25°C.

Table 2: Physicochemical adsorption of Adsorbed dyes by (MC/Zn-NPS) chelating fibers.

| Fiber | Langmuir isotherm constants | | |
|-----------------|-------------------------------|--------------|-------|
| | K_L (L/g) | q_m (mg/g) | R^2 |
| MC/Zn-NPS / M.B | 14×10^{-2} | 175 | 0.998 |
| MC/Zn-NPS/ C.V | 15×10^{-2} | 156 | 0.996 |
| MC/Zn-NPS/ M.G | 18×10^{-2} | 149 | 0.987 |
| Fiber | Freundlich isotherm constants | | |
| | K_F | n | R^2 |
| MC/Zn-NPS / M.B | 13.374 | 2.7 | 0.977 |
| MC/Zn-NPS / C.V | 16.74 | 2.6 | 0.955 |
| MC/Zn-NPS / M.G | 14.362 | 2.4 | 0.842 |

3.2.5. The effect of temperature on the ability for adsorption

Organic dye adsorption was investigated at a range of temperatures (20 to 50°C), as demonstrated in Fig. 10 at pH 6 after four hours. Adsorbed dyes adsorption by MC/Zn-NPs adsorbent was measured using the following parameters: free energy parameter (ΔG°_{ads}), heat of enthalpy parameter (ΔH°_{ads}), and adsorption entropy parameter (ΔS°_{ads}). ΔG°_{ads} parameter was calculated from the following equations Eq6, Eq7, and Eq8.

$$K_C = C_{ads} / C_e \quad \text{Eq. (5)}$$

$$\Delta G^{\circ}_{ads} = -(RT \ln K_C) \quad \text{Eq. (6)}$$

$$\ln K_C = \Delta S^{\circ}_{ads} / R - \Delta H^{\circ}_{ads} / RT \quad \text{Eq. (7)}$$

where C_e is the adsorbed dyes concentration at equilibrium (ppm), C_{ads} is the adsorbed dyes concentration taken by the MC/Zn-NPs material at stability (mg/g), and R is the universal gas constant. K_C is a thermodynamic equilibrium constant.

The plot of $\ln K_C$ vs. $1/T$ was used to determine the remaining parameters (ΔH°_{ads}) and ΔS°_{ads} , with the slope equaling ($-\Delta H^{\circ}_{ads} / R$) and the intercept equal to ($\Delta S^{\circ}_{ads} / R$). The experimental results shown in Table 3 indicate a negative ΔG°_{ads} value, indicating that the process of adsorbed dyes in the MC/Zn-NPs material is spontaneous. Furthermore, it was noted that the exothermic nature of the adsorbed dyes' adsorption by the MC/Zn-NPs material was confirmed by the negative ΔH°_{ads} value. The negative ΔS°_{ads} value showed that Adsorbed dyes solution onto MC/Zn-NPs surface leads to lower disorder and higher

arrangement. Finally, the exothermic nature of the dyes uptake process was confirmed by the calculated ΔH°_{ads} . The values of $\Delta H^{\circ}_{ads} < 8$ kJ/mol is representative of physical sorption and $\Delta H^{\circ}_{ads} > 8-16$ kJ/mol is due to chemical sorption [14,15]. For adsorption of

dyes on MC/Zn-NPs, the values of ΔH°_{ads} is found above 8, so adsorption of dyes on MC/Zn-NPs occurred on the surface by chemical bonding between sorbent and sorbate.

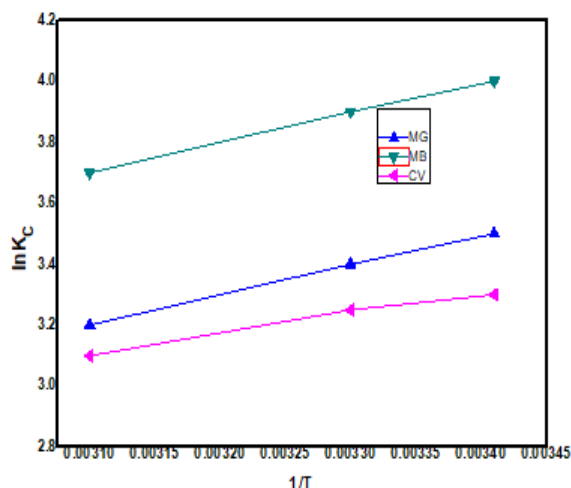


Fig.10: Plot of $\ln K_C$ as a purpose of ($1/T$) absolute temperature for the adsorption of dyes solutions.

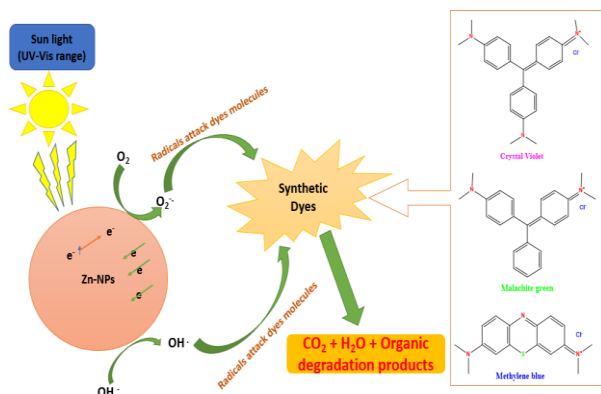
Table 3: Temperature-dependent parameters for adsorption of dye on MC/Zn-NPs.

| System | T (k) | K_C | ΔG°_{ads} (KJ/mol) | ΔH°_{ads} (KJ/mol) | ΔS°_{ads} (J/mol K) |
|-----------------|-------|-------|-----------------------------------|-----------------------------------|------------------------------------|
| MC/Zn-NPS / M.B | 293 | 313 | 15.7 | -44.256 | -55.782 |
| | 303 | 300 | 14.5 | | |
| | 313 | 295 | 17.9 | | |
| MC/Zn-NPS/ C.V | 293 | 298 | 18.5 | -33.653 | -45.452 |
| | 303 | 288 | 17.8 | | |
| | 313 | 279 | 17.6 | | |
| MC/Zn-NPS/ M.G | 293 | 302 | 18.2 | -21.142 | -35.375 |
| | 303 | 295 | 17.5 | | |
| | 313 | 288 | 18.6 | | |

3.3. Mechanism of photocatalytic degradation of MB, CV and BG dyes

The mechanism shown in Schemes 2 can be used to suggest a photocatalytic degradation process. In summary, the formation of electron-hole pairs results from the migration of electrons from the valance band to the conduction band carried on by solar radiation. Hydroxyl radicals (OH) and anion radicals

(O₂⁻) derived from H₂O and O₂, respectively, are examples of active species. The combination of the positive holes and the negative electrons produces these active species. These active species are in charge of breaking down the molecules of MB, CV, and BG into smaller molecules, CO₂ and H₂O, along with the positive holes (h⁺).



Scheme 2: The proposed reaction of photocatalytic degradation of MB, CV and MG dyes.

The adsorption process frequently aids in the combined physisorption and chemisorption processes. Electrostatic interactions between the negative surfaces of adsorbents, which are usually rich in groups that transfer electrons, such as hydroxyl and carbonyl groups, and the positive charges of cationic dyes cause adsorption to occur. The physisorption mechanism is the name given to this activity. In contrast, the chemisorption process is explained by ion exchange or chelation interaction one.

Table 4: Dyes solutions were repeatedly adsorbed.

| Cycle number (DAC/Zn-NPs) | Recovery (%) | | |
|---------------------------|--------------|----|----|
| | CV | MB | MG |
| 1 | 92 | 91 | 90 |
| 2 | 66 | 71 | 77 |
| 3 | 56 | 66 | 66 |
| 4 | 54 | 55 | 56 |
| 5 | 47 | 43 | 49 |

3.4. Desorption and reusability studies

Table 4 shows the desorption of dye solution onto MC/Zn-NPs at various doses of 0.1 M of K₂CO₃ as an eluting agent. Under ideal conditions, the reusability of the polymer at room temperature for MC/Zn-NPs material was investigated for a total of five cycles of

sorption-desorption sequences. Table 4 shows that the MC/Zn-NPs has a high sorption efficiency (more than 92% after five cycles).

3.5. Application on real samples

Water samples analysis was used for offered method accuracy confirmation. From the experimental results that present in table (5), It was noted that MC/Zn-NPS is a good sorbent for added dyes solution concentration.

Table 5: investigation of altered samples using novel sorbent MC/Zn-NPs.

| Wastewater sample's locations | Adsorbent dyes | Added (ppm) | Remaining (ppm) | Recovery (%) | RSD |
|-------------------------------|----------------|-------------|-----------------|--------------|-----|
| Mansoura | M.B | 100 | 97.3 | 97.3 | 1.1 |
| Sinbellawin | | 100 | 96.3 | 96.3 | 1.2 |
| Mokataa | | 100 | 95.2 | 95.2 | 1.1 |
| Mansoura | C.V | 110 | 101.9 | 91.8 | 1.2 |
| Sinbellawin | | 110 | 99.2 | 90.1 | 1.1 |
| Mokataa | | 110 | 103.4 | 94 | 19 |
| Mansoura | M.G | 150 | 142 | 94 | 2.2 |
| Sinbellawin | | 150 | 143 | 95.3 | 2.4 |
| Mokataa | | 150 | 144 | 96 | 1.2 |

Table 6: Study of the equilibrium times for the dyes under study using different adsorbents.

| Adsorbates | Adsorbents | Sorption capacity (mg/g) | Reference |
|-------------------------------|------------------------------------------|--------------------------|------------------|
| CV dye | Nanocomposite | 28.2 | [11] |
| | Red mud | 60.5 | [12] |
| | Activated carbon | 67.1 | [13] |
| | Kaolinite | 129.8 | [14] |
| | HDTMA-bentonite | 162.5 | [15] |
| MB dye | CuGA 90-2.2 | 124.6 | [16] |
| | UiO-66 | 91.0 | [17] |
| | Fe3O4@MIL-100 | 56.1 | [18] |
| | MIL-101 | 21.7 | [18] |
| | NH2-MIL-88B | 61.4 | [19] |
| Bentonite | Malachite Green | 7.716 | [20] |
| Crude And Purified Clay | Methylene Blue | 50 and 68,5 | [21] |
| Natural Clay | Nile Blue And Brilliant Cresyl Blue | 25 and 42 | [22] |
| Cu(II)-Loaded Montmorillonite | Crystal Violet | 114 | [23] |
| Natural Clay | Neutral Red, Methyl Violet, Methyl Green | 567, 526, 427 and 300 | [24] |
| Sawdust | Malachite, Crystal violet and green dye | 240, 170, and 230 | Current research |

Comparison of the proposed adsorbent with other cited adsorbents with great extraction efficiency and precision, the suggested adsorbent can be used to recover and separate adsorbed dyes from various materials.

The performance of the current adsorbent is compared to other adsorbents that have previously been reported in the literature in Table 6. When studying different adsorbents for

the separation of MC/Zn-NPs, both the amount of sorption and the kind of sample matrices employed for the separation should be considered. Table 6 demonstrates that, in comparison to other adsorbents, the current adsorbent has comparatively high capacities for the recovery of adsorbed dyes.

4. Conclusions

Cellulose that was extracted from hardwood was subjected to sodium hydroxide treatment and potassium periodate oxidation in order to produce the appropriate C-2/C-3 DAC. Through a reductive process, zinc nanoparticles were grafted onto oxidized hardwood (DAC) with the addition of ZnNO₃. This produced MC/Zn-NPs. The removal of cationic dyes is enhanced by the carboxylic groups present on MC/Zn-NPs. The removal of cationic dyes is enhanced by the carboxylic groups present in MC/Zn-NPs. The FT-IR research and analyses verified the emergence of new groups and surface structure alterations. Adsorbent dosage, contact duration, and starting dye solution concentration all affected the percentage of removal, whereas pH significantly affected MC/Zn-NPs Zeta potential.

5. References

1. Liu, C. *et al.* (2020) Research and Development on Therapeutic Agents and Vaccines for COVID-19 and Related Human Coronavirus Diseases. *ACS Cent. Sci.* **6**, 315–331.
2. Malachova, A. *et al.* (2013) Collaborative investigation of matrix effects in mycotoxin determination by high performance liquid chromatography coupled to mass spectrometry. *Qual. Assur. Saf. Crop. Foods* **5**, 91–103.
3. O'Connell, D. W., Birkinshaw, C. & O'Dwyer, T. F. (2008) Heavy metal adsorbents prepared from the modification of cellulose: A review. *Bioresour. Technol.* vol. **99** 6709–6724 (Bioresour Technol.).
4. Monier, M., Bukhari, A. A. H. & Elsayed, N. H. (2020) Designing and characterization of copper (II) ion-imprinted adsorbent based on isatin functionalized chitosan. *Int. J. Biol. Macromol.* **155**, 795–804.
5. Šćiban, M., Klačnja, M. & Škrbić, B. (2006) Modified softwood sawdust as adsorbent of heavy metal ions from water. *J. Hazard. Mater.* **136**, 266–271.
6. Chaves, F. A. & Jiménez, D. (2018) Electrostatics of two-dimensional lateral junctions. *Nanotechnology* **29**, 275203.
7. Setyono, D. & Valiyaveetil, S. (2014) Chemically modified sawdust as renewable adsorbent for arsenic removal from water. *ACS Sustain. Chem. Eng.* **2**, 2722–2729.
8. Jin, L., Li, W., Xu, Q. & Sun, Q. (2015) Amino-functionalized nanocrystalline cellulose as an adsorbent for anionic dyes. *Cellulose* **22**, 2443–2456.
9. Ahmad, T. *et al.* (2010) Removal of pesticides from water and wastewater by different adsorbents: A review. *J. Environ. Sci. Heal. - Part C Environ. Carcinog. Ecotoxicol. Rev.* **28**, 231–271.
10. Zhang, M., Zhang, Y. & Helleur, R. (2015) Selective adsorption of Ag⁺ by ion-imprinted O-carboxymethyl chitosan beads grafted with thiourea-glutaraldehyde. *Chem. Eng. J.* **264**, 56–65.
11. Xu, Y., Huang, C. & Wang, X. (2013) Characterization and controlled release aloe extract of collagen protein modified cotton fiber. *Carbohydr. Polym.* **92**, 982–988.
12. Monier, M., Youssef, I. & El-Mekabaty, A. (2019) Preparation of functionalized ion-imprinted phenolic polymer for efficient removal of copper ions. *Polym. Int.* **69**, 31–40.
13. Yusof, N. F., Mehamod, F. S. & Mohd Suah, F. B. (2019) Fabrication and binding characterization of ion imprinted polymers for highly selective Co²⁺ ions in an aqueous medium. *J. Environ. Chem. Eng.* **7**, 103007.
14. Varma, A. J. & Kulkarni, M. P. (2002) Oxidation of cellulose under controlled conditions. *Polym. Degrad. Stab.* **77**, 25–27.
15. Chaves, F. A. & Jiménez, D. (2018) Accepted Manuscript. *Nanotechnology* **29**.
16. Ganapathy Selvam, G. & Sivakumar, K. (2015) Phycosynthesis of silver nanoparticles and photocatalytic degradation of methyl orange dye using silver (Ag) nanoparticles synthesized from

-
- Hypnea musciformis (Wulfen) J.V. Lamouroux. *Appl. Nanosci.* **5**, 617–622.
17. Bharti *et al.* (2022) A review on the capability of zinc oxide and iron oxides nanomaterials, as a water decontaminating agent: adsorption and photocatalysis. *Appl. Water Sci.* **12**, 1–14.
 18. Rafeaie, H. A., Nor, R. M., Azmina, M. S., Ramli, N. I. T. & Mohamed, R. (2017) Decoration of ZnO microstructures with Ag nanoparticles enhanced the catalytic photodegradation of methylene blue dye. *J. Environ. Chem. Eng.* **5**, 3963–3972.
 19. Jin, L., Li, W. & Xu, Q. Amino-(2015) functionalized nanocrystalline cellulose as an adsorbent for anionic dyes. *Cellulose* doi:10.1007/s10570-015-0649-4.
 20. Gholami, M., Vardini, M. T. & Mahdavinia, G. R. (2016) Investigation of the effect of magnetic particles on the Crystal Violet adsorption onto a novel nanocomposite based on κ -carrageenan-g-poly(methacrylic acid). *Carbohydr. Polym.* **136**, 772–781.
 21. Zhang, L., Dou, S. X., Liu, H. K., Huang, Y. H. & Hu, X. L. (2016) Symmetric electrodes for electrochemical energy-storage devices. *Adv. Sci.* **3**,.
 22. Hamidzadeh, S., Torabbeigi, M. & Shahtaheri, S. J. (2015) Removal of crystal violet from water by magnetically modified activated carbon and nanomagnetic iron oxide. *J. Environ. Heal. Sci. Eng.* **13**, 1–7.
 23. Chen, Z. *et al.* (2013) Multifunctional kaolinite-supported nanoscale zero-valent iron used for the adsorption and degradation of crystal violet in aqueous solution. *J. Colloid Interface Sci.* **398**, 59–66.
 24. Anirudhan, T. S. & Ramachandran, M. (2015) Adsorptive removal of basic dyes from aqueous solutions by surfactant modified bentonite clay (organoclay): Kinetic and competitive adsorption isotherm. *Process Saf. Environ. Prot.* **95**, 215–225.